View metadata, citation and similar papers at core.ac.uk
brought to you by CORE
provided by Elsevier - Publisher Connector

Thin Solid Films 583 (2015) 55–59

Contents lists available at ScienceDirect

Thin Solid Films

journal homepage: www.elsevier.com/locate/tsf

Amorphous thin GeSbTe phase-change films prepared by radical-assisted metal-organic chemical vapor deposition

Yoshihisa Fujisaki *, Yoshitaka Sasago, Takashi Kobayashi

Central Research Laboratory, Hitachi, Ltd., 1-280 Higashi-Koigakubo, Kokubunji, Tokyo 185-8601, Japan

ARTICLE INFO

Article history:
Received 28 April 2014
Received in revised form 16 March 2015
Accepted 16 March 2015
Available online 24 March 2015

Keywords:
Phase change
Metal organic chemical vapor deposition
Non-volatile memory
Chalcogenide
Germanium–antimony–tellurium
Three-dimensional structures

ABSTRACT

Amorphous thin $Ge_2Sb_2Te_5$ films were deposited by MOCVD (metal organic chemical vapor deposition) on three-dimensional structures. Ammonium gas, used as a reactant, reduced the deposition temperature to 150 °C, which is lower than that of metal-organic precursors. Introducing nitrogen and hydrogen radicals made by decomposition of the ammonium gas further reduced the growth temperature. The lowest growth temperature producing a realistic growth rate was 100 °C. Phase-change memory cells made of MOCVD-grown films were confirmed to have operation and reliability characteristics as good as those of conventional cells made of sputter-deposited films.

© 2015 Central Research Laboratory, Hitachi, Ltd. Published by Elsevier B.V. This is an open access article under the CC BY-NC-ND license (http://creativecommons.org/licenses/by-nc-nd/4.0/).

1. Introduction

Phase-change memory (PCM) is one of the most-promising technologies for mass-storage-class non-volatile applications. Currently, NAND flash memories are used in solid-state drives that are replacing HDDs (hard-disk drives) for applications requiring relatively small memory capacity. However, it is expected that the memory capacity of NAND flash memories cannot catch up to that of HDDs because of the scaling limit imposed on a NAND memory cell [1,2]. To overcome this problem, 3D (three-dimensional) NAND flash memories have been proposed [3–5], and some of them are nearing production.

Our group previously proposed a 3D PCM that is superior to 3D NAND flash memories in terms of both scaling limit and operation speed [6]. Similar to 3D NAND flash memories, 3D PCM has an array of memory cells in the vertical direction of a memory chip. This array is fabricated on the side wall of a hole, the diameter of which can be reduced to the lithography limit, in the chip. To fabricate this structure, therefore, thin and smooth phase-change films should be deposited uniformly on the side wall of deep and small holes.

Chemical vapor deposition is thought to be the most suitable technique for creating this 3D memory structure. Germanium–antimony–tellurium (GeSbTe) films deposited by MOCVD (metal-organic chemical vapor deposition) have been reported by several groups [7–10]; however, most of these films have rough and irregular surfaces because they crystallize during the deposition process. Since the decomposition temperatures of metal-organic precursors are above 260 °C in general, the film-deposition temperatures used were around 300 °C. Because the crystallization temperature of GeSbTe is approximately 150 °C [11], GeSbTe films deposited above this temperature will be crystallized and have rough surfaces.

In this study, the deposition temperature of GeSbTe films was reduced by enhancing decomposition of precursors both in vapor phase and on a solid surface. Unlike films deposited by conventional MOCVD techniques, GeSbTe films were deposited at temperatures lower than the decomposition temperatures of precursors by introducing additional reactants. The resulting amorphous $Ge_2Sb_2Te_5$ films have smooth surfaces suitable for 3D PCMs.

2. Experimental details

The metal-organic precursors used in this study were (N, N′-diisopropyl-dimethylguanidyl)(dimethylamino)germanium (II), tris(dimethylamino)antimony, and (tert-buthyl)(2-propenyl)tellurium supplied by Tri Chemical Laboratories Inc. Their approximate decomposition temperatures are 205 °C, 316 °C, and 200 °C, respectively. All of them are liquid at room temperature, so they were introduced into a CVD reactor by bubbling nitrogen carrier gas into precursor storage bottles. Ammonia was also introduced into the reactor to enhance film deposition at low temperature (since it enables deposition below 200 °C). In some cases, the ammonia was decomposed by a heated platinum wire, in a remote chamber connected to the main reactor, prior to being fed into the reactor.

* Corresponding author at: 1-280 Higashi-koigakubo, Kokubunji, Tokyo 185-8601, Japan.
E-mail address: yoshihisa.fujisaki@yourfriend.tokyo (Y. Fujisaki).

http://dx.doi.org/10.1016/j.tsf.2015.03.034
0040-6090/© 2015 Central Research Laboratory, Hitachi, Ltd. Published by Elsevier B.V. This is an open access article under the CC BY-NC-ND license (http://creativecommons.org/licenses/by-nc-nd/4.0/).

All the gases were introduced separately into a shower head set in the reactor chamber and mixed before reaching the surface of a sample substrate. The total vapor pressure of the reactor was kept at 400 Pa in all cases. The composition of the deposited GeSbTe film was adjusted to be $Ge_2Sb_2Te_5$ by controlling the flow rate of the metal-organic precursors. The film composition was confirmed by inductively coupled plasma mass analysis of 50-nm-thick films deposited on SiO_2.

The deposited films were evaluated by using relatively thick (namely, greater than 20 nm) films, whereas the thickness of $Ge_2Sb_2Te_5$ used in practical 3D PCMs is less than 5 nm. To obtain these thick films, higher growth rates were used. The substrate temperature was fixed at 150 °C when decomposed ammonia, with which smooth amorphous $Ge_2Sb_2Te_5$ can be deposited, was used. Under this condition, the growth rate of the films was 0.2 nm/min.

The thickness of the deposited films was confirmed by cross-sectional TEM (transmission electron microscope) (model HD-2700 (200 kV), Hitachi High-Technologies) and secondary electron microscope (model S-5000 (5 kV), Hitachi Ltd.). The sample for TEM was prepared by focused ion beam thinner. The observation area was made as thin as 100 nm.

Chemical bonds of nitrogen were analyzed by XPS (X-ray photoelectron spectroscopy). Model HAC5000 made by VSW Atomtech Ltd. was used for XPS analysis. The X-ray source was aluminum Kα. The take-off angle of photoelectrons was set to 65°. XPS analysis was performed without sputtering cleaning to prevent the effect of the cleaning on the composition of the deposited films. The binding-energy scale was referenced to the position of the Ag 3d peak (368.27 eV). The software for peak fitting was written in-house. The raw data peaks were decomposed by a 50%-Gaussian/50%-Lorentzian mixed function with Shirley background.

The crystallinity of deposited films was evaluated by XRD (X-ray diffraction). XRD patterns were obtained by model M21X, MAC Science with theta–2theta mode. The X-ray source was copper.

To evaluate the performances as a PCM device, current-induced phase-change characteristics were investigated by using a test device in which a 50-nm-thick $Ge_2Sb_2Te_5$ film was sandwiched between a cylindrical bottom electrode and a thin top electrode having a larger area than that of the bottom electrode. The diameter of the bottom electrode was 170 nm, and the thickness of the top electrode was 50 nm. Both electrodes were made of tungsten.

The electrical characteristics of the $Ge_2Sb_2Te_5$ films were measured by an Agilent 4156C and an Agilent 81110a. In particular, the resistance of the film was measured by the former, and set and reset pulses were generated by the latter.

To fabricate 3D PCMs, coverage of a film on complex 3D structures should be quite uniform and independent of positions in the structure such as the bottom of a deep hole, the side wall of a narrow groove, and the top surface of the structure. The film coverage was therefore evaluated using a substrate with test 3D structures, which were made in a thermally grown SiO_2 layer on a silicon substrate. To make the test structures, amorphous silicon was used as a hard mask for dry etching because it is difficult to make small and deep holes with photo-resist masks. The 3D structures were covered with thin Al_2O_3 (grown by atomic layer deposition) to unify the surface energy of the structures.

Surface roughness of films was evaluated using a non-contact-mode AFM (atomic force microscope) (model XE150, Park Systems). Since the roughness of a film will be affected by that of the underlying substrate, SiO_2 thermally grown on silicon was used as a substrate. The RMS (root mean square) roughness of this substrate was confirmed to be small, i.e., 0.17 nm.

3. Deposition of $Ge_2Sb_2Te_5$

The relationship between reciprocal temperature and deposition rate of a $Ge_2Sb_2Te_5$ film is shown in Fig. 1. The square plots correspond to data obtained with thermally decomposed ammonia, and the other plots correspond to data obtained with non-decomposed ammonia. The mole flow rates of the germanium, antimony, and tellurium precursors were fixed to 4.6×10^{-8}, 8.0×10^{-7}, and 1.3×10^{-5} mole/min, respectively. Before Fig. 1 is discussed in detail, the decomposition characteristics of ammonia (decomposed by using a heated platinum wire) are discussed first. It was reported that platinum works as a catalyst for NH_3 decomposition very efficiently if it is heated to above 700 °C [12,13].

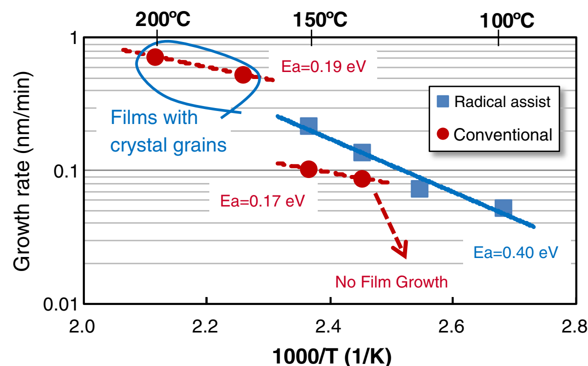

Fig. 1. Relationship between $Ge_2Sb_2Te_5$ film growth rate and reciprocal temperature during film growth. The square dots correspond to data obtained with thermally decomposed ammonia (radical-assisted mode), and the other dots correspond to data obtained with non-decomposed ammonia (conventional mode).

To investigate the decomposition characteristics by platinum catalysis quantitatively, (001)-oriented bare silicon substrates were nitrified in a MOCVD chamber. Temperature dependence of averaged concentration of nitrogen in the silicon substrate (probed by XPS very near to the surface) is shown in Fig. 2. Temperature of the platinum wire was kept at 700 °C, and processing time was kept to 30 min. The concentration of nitrogen in the silicon substrates was evaluated by XPS. The nitrogen 1s peak shown in Figs. 3(a) and (b) was assigned to be nitrogen having a chemical bond with a silicon atom. As for the samples processed at 200 °C, in addition to the nitrogen 1s peak, another peak was detected in the XPS spectra. According to Ref. [14], this peak was assigned to be nitrogen in an organic matrix (Fig. 3(b)). Below 150 °C, the nitrogen 1s peak disappeared, and only the peak assigned to be that nitrogen remained. The silicon substrate was therefore not nitrided below 150 °C. In spite of the background noise, the peaks in Figs. 3(a) and (b) can be assigned to the nitrogen 1s peak and the peak of the nitrogen in an organic matrix, respectively, because their positions correspond to previously reported data [14]. Only nitrogen atoms having a Si – N bond are taken into account in the plots in Fig. 2. It is obvious from Fig. 2 that nitridation of bare silicon takes place at temperatures higher than 150 °C and saturates at 400 °C. Because nitridation was not observed

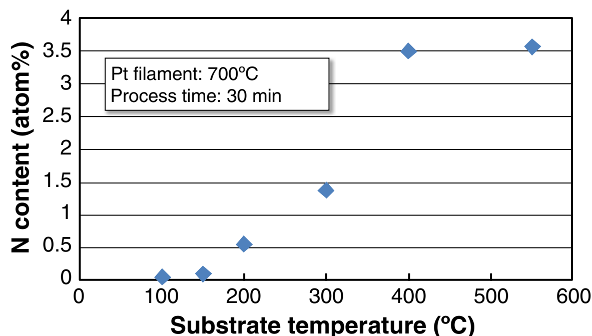

Fig. 2. Nitridation characteristics for nitrogen radicals made from thermally decomposed ammonia. Platinum wire kept at 700 °C was used as a catalyst for ammonia decomposition. The plots show the dependence of the amount of nitrogen in silicon on substrate temperature.

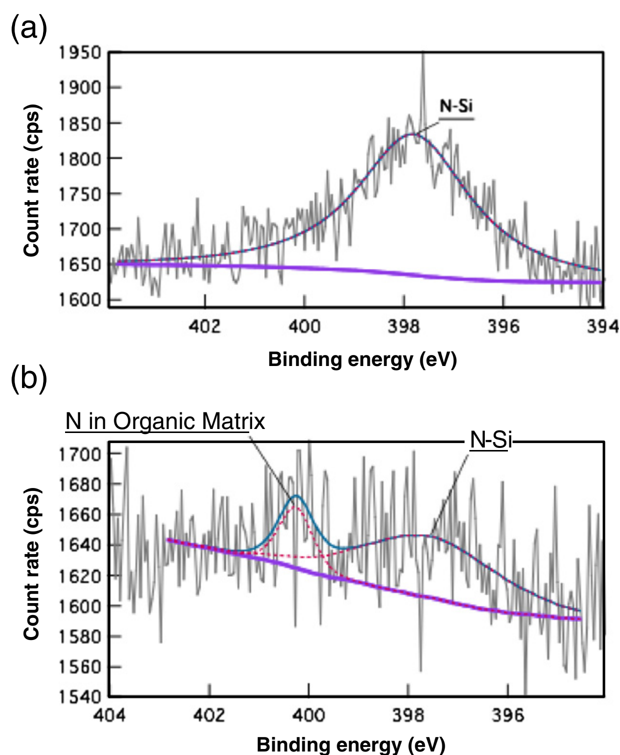

Fig. 3. XPS spectrum corresponding to the N 1s peak assigned to a chemical bond between silicon atoms. Samples (a) and (b) were prepared at 400 °C and 200 °C, respectively.

below 300 °C when the heated platinum wire was not present, the low-temperature nitridation shown in Fig. 2 is supposed to be caused by nitrogen radicals made by a catalytic reaction on the heated platinum wire. The existence of the nitrogen radicals was thus strongly expected. The organic matrix found at low temperature is thought to be formed by the reaction between the nitrogen radicals and residual organics stuck on the MOCVD chamber wall. It is therefore concluded that the nitrogen radicals can react with the organics even at 100 °C.

It is clearly shown in Fig. 1 that growth of a $Ge_2Sb_2Te_5$ film is enhanced by nitrogen radicals. Conventional growth (growth with non-decomposed ammonia) is divided into two modes. At temperature above 170 °C, the films become partially crystallized with a very irregular surface because they were grown at temperature higher than the crystallization temperature of $Ge_2Sb_2Te_5$. On the contrary, the films become amorphous with very smooth surfaces when they were grown at temperature below 150 °C. Of course, the chemical reactions taking place in these two modes are different, so they should be analyzed separately.

Even non-decomposed ammonia increased the deposition rate, because hydrogen atoms decomposed from ammonia enhance the chemical reaction during CVD. Decomposed ammonia produces not only hydrogen but also nitrogen radicals, which enhance the chemical reaction further. The activation energies of conventional growth modes are less than one half of that of growth with decomposed ammonia. Because these activation energies correspond to chemical-reaction energies of film growth, chemicals react more efficiently with each other by using thermal energy in a process with high activation energy. At temperatures between 135 °C and 150 °C, the film growth rate in the case with decomposed ammonia is twice that in the case of the conventional mode (i.e., without decomposed ammonia).

It is also clear from Fig. 1 that the film-growth kinetics in both conventional and radical-assisted modes is called "reaction limited," since these two modes actually have activation energies. If growth rate does not depend on substrate temperature, the growth mode is called "diffusion limited." In diffusion-limited mode, conformal film growth on complex 3D structures becomes impossible because the amount of precursors delivered will not be uniformly distributed across all the surfaces of a 3D structure. On the contrary, if the growth mode is reaction limited, a conformal film can be grown even if the surface of the substrate has a complex structure. It can therefore be said that both growth modes are applicable to fabricating 3D PCMs.

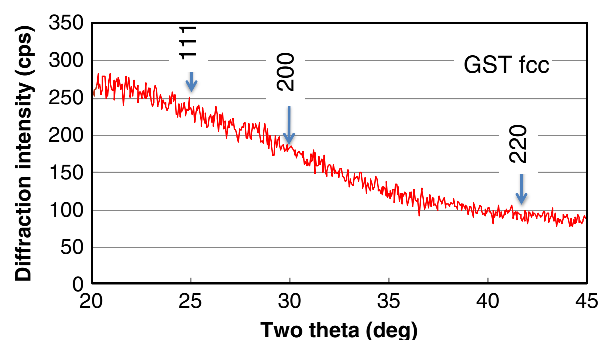

Fig. 4. Typical XRD pattern of $Ge_2Sb_2Te_5$ film grown in radical-assisted mode at 150 °C. Arrows drawn on the spectrum show the positions of peaks for $Ge_2Sb_2Te_5$ having a fcc crystal structure. The absence of peaks at the points indicated by arrows means the film is amorphous.

A typical XRD pattern of a $Ge_2Sb_2Te_5$ film is shown in Fig. 4. The film was deposited at 150 °C by using radical-assisted mode on SiO_2 thermally grown on a silicon substrate. Under this growth condition, approximately 3.5-atom% of nitrogen was incorporated into the $Ge_2Sb_2Te_5$ film. In the XRD pattern, the positions of the diffraction peaks originated from the $Ge_2Sb_2Te_5$ fcc (face-centered cubic) crystal structure are also drawn. Because fcc is the phase of $Ge_2Sb_2Te_5$ with the lowest crystallization temperature, the absence of fcc peaks in the XRD pattern means that this film is amorphous. This perfect elimination of crystal phase might be partially due to the increase in crystallization temperature caused by nitrogen incorporation into the film [15].

The surface morphology, shown in Fig. 5, was obtained by AFM. The sample was the same one used to obtain the XRD pattern shown in Fig. 4. Because the film is confirmed to be amorphous in Fig. 4, no crystal grains exist on the surface in Fig. 5. The RMS value of surface roughness is 0.30 nm. Since the film is smooth enough, it is applicable to practical 3D devices.

To investigate the conformability of a $Ge_2Sb_2Te_5$ film on a substrate with complex 3D structures, the deposited film was observed by TEM. The 3D test structures were fabricated as explained in the experimental section. The smallest diameter of the holes and the smallest width of the grooves were 29 nm and 26 nm, respectively. The same deposition

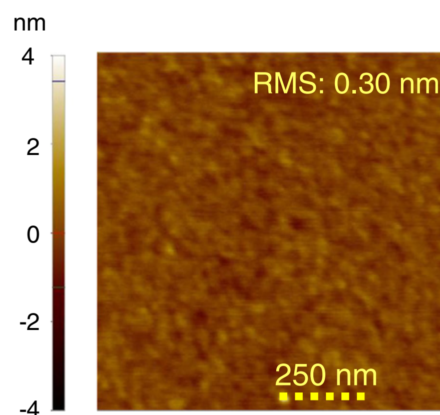

Fig. 5. Typical surface morphology taken by AFM. The film was deposited under radical-assisted mode at 150 °C. The root-mean-square value of the surface roughness was calculated to be 0.30 nm.

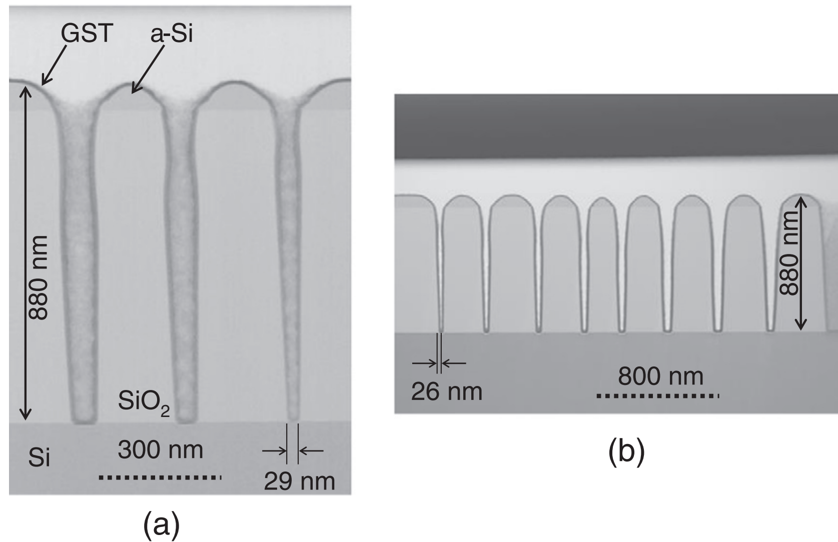

Fig. 6. Cross-sectional TEM images of deep holes (a) and grooves (b). The dark contrast covering the 3D structure is the deposited $Ge_2Sb_2Te_5$ film. The samples were prepared under the same deposition condition used for the samples in Figs. 4 and 5. The diameter and width of the smallest hole and groove are 29 nm and 26 nm, respectively. Coverage indexes of the smallest holes (C_{hole}) and grooves (C_{groove}) are larger than 0.92 and 0.99, respectively.

condition as that used to prepare the samples in the cases of Figs. 4 and 5, except a shorter deposition time was used to obtain a thinner film, was employed. Cross-sectional views of the holes and grooves are shown in Fig. 6(a) and (b), respectively. The highest aspect ratios of a hole and a groove, namely, the ratio between depth and width at the top of each, are 31.5 and 35, respectively. As is clear from the images, very smooth and uniform films, even at the bottoms of the finest hole and groove, were deposited over the whole complex pattern. Coverage index C is defined as the ratio of the film thickness at the bottom (B) and that of the top surface (T); $C = B/T$. The index of the smallest hole (C_{hole}) was calculated to be 0.92, and that of the smallest groove (C_{groove}) exceeds 0.99. Due to the difference between the easiness of process-gas delivery and that of processed-gas venting, C_{hole} is smaller than C_{groove}. However, 0.92 is an acceptable value because the non-uniformity of the thickness of the top surface and that of the bottom of a hole is less than 10%. As described in the introduction, the side wall of the structures is the most-important feature in regard to making 3D PCMs a reality. In light of that fact, the result of the TEM observation indicates that the growth condition (i.e., deposition temperature of 150 °C) is applicable for fabricating 3D PCMs by using a lithography technology node finer than 30 nm.

During the deposition of compound materials on complex 3D patterns, growth abnormalities, such as growth of precipitates, and locally thicker film growth at the corner of holes, are often found at the edge of structures. A typical AFM image of a hole array is shown in Fig. 7. Under radical-assisted mode, 16-nm-thick $Ge_2Sb_2Te_5$ was deposited at 150 °C. No abnormal growth can be seen at the corner of holes. Apparently, precipitates were also perfectly eliminated by growth of an amorphous film at low temperature.

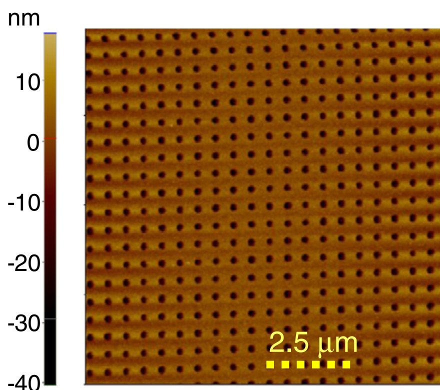

Fig. 7. Surface of hole-array area observed by AFM. The sample was the same one used in the case of Fig. 6. Neither abnormal growth nor precipitation can be seen.

4. Electrical properties

The electrical properties of the deposited films were investigated by using 50-nm-thick films grown at 150 °C under radical-assisted mode. A current passing across the film was used to drive the test memory cells, whereas a current passing parallel to the film surface will be used to drive actual 3D memory cells (as explained in the introduction). This simplified device structure can be used to obtain reliable electrical-property data with high reproducibility.

A typical current-pulse response of a test memory cell is shown in Fig. 8. The horizontal and vertical axes correspond to the voltage applied to the $Ge_2Sb_2Te_5$ film (V_{GST}) and the resistivity of the film, respectively. Because PCM cells are operated by current pulses, V_{GST} was measured during the current-pulse application. Current-pulse width was 50 ns with 5-ns raise and trailing times. Initially, the film was highly resistive

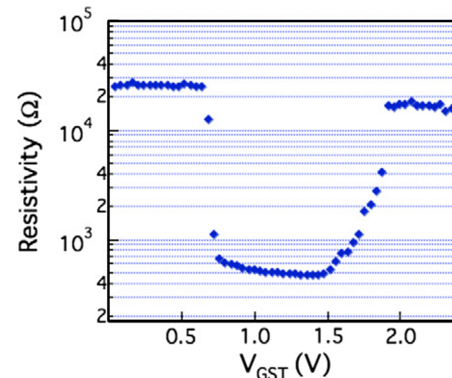

Fig. 8. Typical pulse response of a phase-change memory cell made of MOCVD-grown $Ge_2Sb_2Te_5$ film. The film was deposited at 150 °C in radical-assisted mode. The thickness of the film was 50 nm, and the diameter of the bottom electrode of the memory cell was 170 nm. The current pulse used to obtain the characteristics was 50 ns in width with raise and trailing times of 5 ns. V_{GST} is the measured voltage applied between the top and bottom electrodes during the current-pulse applications.

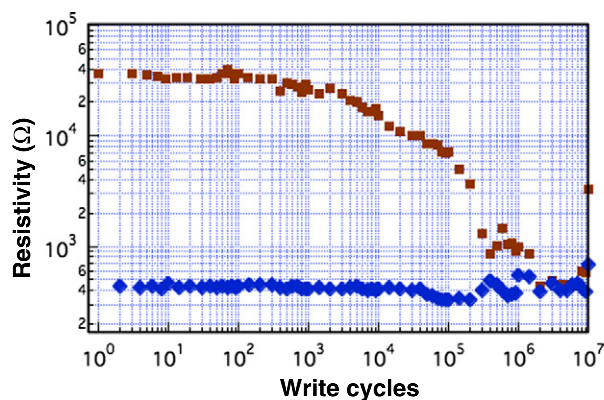

Fig. 9. Endurance property of the same memory cell used in the case of Fig. 8. Set pulses were controlled to be 1.2 V in height and 15 ns in width with 5-ns raise and trailing times. Reset pulses were 2.0 V in height and 50 ns in width with 5-ns raise and trailing times. The ratio of resistivities in set and reset states was kept above 10 up to 10^5 cycle pulses.

("reset state"), but it changed to low resistive state ("set operation") when current pulses were applied while the pulse height was raised in a stepwise manner. In this case, the set voltage was found to be 0.5 V. Under continual application of current pulses while the pulse height was raised, the device changed from this state ("set state") to highly resistive state again ("reset operation") at approximately 1.5 V. The ratio of the resistivities in the set and reset states is large, i.e., 20, which is high enough for a PCM cell. The operational speed and voltage of the memory cell are also acceptable for highly dense memories such as terra-bit-scale ones.

The endurance characteristics of the test memory cell are shown in Fig. 9. The current-pulse widths for setting and resetting the memory cell are 50 and 5 ns, respectively. The set and reset current pulses were selected to give V_{GST} of 1.2 and 2.0 V, respectively. From a few-thousand cycles of current pulses, the reset state gradually degraded to a lower resistive state. However, the resistivity ratio of the memory cell stayed above 10 up to 10^5 pulse cycles. This endurance characteristic was confirmed to be as good as that of a control sample made of sputter-deposited films. It can therefore be concluded that the MOCVD-grown $Ge_2Sb_2Te_5$ film has enough quality in terms of electrical performance to be applied to practical PCMs.

5. Summary

Amorphous $Ge_2Sb_2Te_5$ thin films were grown by MOCVD at a temperature below the decomposition temperature of metal-organic precursors. With the help of nitrogen and hydrogen radicals made from thermally decomposed ammonia, the films can be deposited even at 100 °C. The deposited films have smooth surfaces, namely, RMS roughness of 0.30 nm, even on a substrate with complex three-dimensional structures. The step coverage of the films on complex 3D structures was investigated. Specifically, when the thickness at the bottom of a 29-nm-diameter hole was compared to that at the top surface, it was found that the non-uniformity of film thickness was less than 10%. Moreover, when the thickness at the bottom of a 26-nm-wide groove and that at the top surface were compared, it was found that the non-uniformity of the film thickness was less than 1%.

Phase-change memory cells made of MOCVD-grown films demonstrated switching performance as good as that of similar cells made of sputter-deposited films. It is therefore concluded that MOCVD-grown amorphous films can be employed to fabricate highly dense three-dimensional phase-change memories.

Acknowledgments

The authors express our sincere thanks to the staff of the Storage Technology Research Center and the Electronic Research Center, Central Research Laboratory, Hitachi, Ltd., for their cooperation.

References

[1] Y. Fujisaki, Review of emerging new solid-state non-volatile memories, Jpn. J. Appl. Phys. 52 (2013) 040001.
[2] Y. Fujisaki, Current status of nonvolatile semiconductor memory technology, Jpn. J. Appl. Phys. 49 (2010) 100001.
[3] H. Tanaka, M. Kido, K. Yahashi, M. Oomura, R. Katsumata, M. Kito, Y. Fukuzumi, M. Sato, Y. Nagata, Y. Matsuoka, Y. Iwata, H. Aochi, A. Nitayama, Bit cost scalable technology with punch and plug process for ultra high density flash memory, Proc. Int. Symp. VLSI Technology 2007, p. 14.
[4] J. Jang, H.-S. Kim, W. Cho, H. Cho, J. Kim, S.I. Shim, Y. Jang, J.-H. Jeong, B.-K. Son, D.W. Kim, K. Kim, J.-J. Shim, J.S. Lim, K.-H. Kim, S.Y. Yi, J.-Y. Lim, D. Chung, H.-C. Moon, S. Hwang, J.-W. Lee, Y.-H. Son, U.-I. Chung, W.-S. Lee, Vertical cell array using TCAT (terabit cell array transistor) technology for ultra high density NAND flash memory, Proc. Int. Symp. VLSI Technology 2009, p. 192.
[5] H.-T. Lue, T.-H. Hsu, Y.-H. Hsiao, S.P. Hong, M.-T. Wu, F.-H. Hsu, N.Z. Lien, S.-Y. Wang, J.-Y. Hsieh, L.-W. Yang, T. Yang, K.-C. Chen, K.-Y. Hsieh, C.-Y. Lu, A highly scalable 8-layer 3D vertical-gate (VG) TFT NAND flash using junction-free buried channel BE-SONOS device, Proc. Int. Symp. VLSI Technology 2010, p. 131.
[6] M. Kinoshita, Y. Sasago, H. Minemura, Y. Anzai, M. Tai, Y. Fujisaki, S. Kusaba, T. Morimoto, T. Takahama, T. Mine, A. Shima, Y. Yonamoto, T. Kobayashi, Scalable 3-D vertical chain-cell-type phase-change memory with 4 F2 poly-Si diodes, VLSI Technology 2012, p. 35.
[7] R.-Y. Kim, H.-G. Kim, S.-G. Yoon, Structural properties of $Ge_2Sb_2Te_5$ thin films by metal organic chemical vapor deposition for phase change memory applications, Appl. Phys. Lett. 89 (2006) 102107.
[8] J.F. Zheng, J. Reed, C. Schell, W. Czubatyj, R. Sandoval, J. Fournier, W. Li, W. Hunks, C. Dennison, S. Hudgens, T. Lowrey, MOCVD $Ge_3Sb_2Te_5$ for PCM applications, IEEE Electron Device Lett. 31 (2010) 999.
[9] J.F. Zheng, P. Chen, W. Hunks, W. Li, J. Cleary, J. Reed, J. Ricker, W. Czubatyj, C. Schell, R. Sandoval, S. Hudgens, C. Dennison, T. Lowrey, MOCVD GST for high speed and low current phase change memory, Non-volatile Memory Symposium 2011, p. 9.
[10] Kohei Suda, Tomohiro Uno, Tatsuya Miyakawa, Naomi Sawamoto, Hideaki Machida, Masato Ishikawa, Hiroshi Sudoh, Yoshio Ohshita, Atsushi Ogura, $Ge_2Sb_2Te_5$ film fabrication by tellurization of chemical vapor deposited GeSb, Jpn. J. Appl. Phys. 52 (2013) 128006.
[11] T.P.L. Pedersen, J. Kalb, W.K. Njoroge, D. Wamangi, M. Wuttig, F. Spaepen, Mechanical stresses upon crystallization in phase change materials, Appl. Phys. Lett. 79 (2001) 3597.
[12] S.F. Yin, B.Q. Xu, X.P. Zhou, C.T. Au, A mini-review on ammonia decomposition catalysts for on-site generation of hydrogen for fuel cell applications, Appl. Catal. A Gen. 277 (2004) 1.
[13] G. Papapolymerou, V. Bontozoglou, Decomposition of NH_3 on Pd and Ir comparison with Pt and Rh, J. Mol. Catal. A Chem. 120 (1997) 165.
[14] J.F. Moulder, W.F. Stickle, P.E. Sobol, K.D. Bomben, Handbook of X-ray Photoelectron Spectroscopy, Perkin-Elmer Co., 1992
[15] I.-M. Park, T.-Y. Yang, S.W. Jung, Y.K. Kim, H. Horii, Y.-C. Joo, Investigation of crystallization behaviors of nitrogen-doped $Ge_2Sb_2Te_5$ films by thermomechanical characteristics, Appl. Phys. Lett. 94 (2009) 061904.